JOURNAL OF PROPULSION AND POWER
Vol. 17, No. 1, January–February 2001

Flame Spread with Sudden Expansions of Ports of Solid Propellant Rockets

B. N. Raghunandan*
Indian Institute of Science, Bangalore 560 012, India
and
V. R. Sanal Kumar,† C. Unnikrishnan,‡ and C. Sanjeev§
Indian Space Research Organization, Trivandrum 695 022, India

Detailed theoretical and experimental studies on flame spread over nonuniform ports of solid propellant rockets have been carried out. An idealized two-dimensional laboratory motor was used for the experimental study with the aid of cinematography. A detailed numerical simulation of the flame spread has also been carried out with the help of a two-dimensional Navier–Stokes solver. Experimental results showing the phenomenon of secondary ignition have been reported earlier and also reviewed here with the inclusion of additional results of a three-dimensional geometry closer to a dual-thrust motor. In this paper more tangible results including the numerical modeling of flame spread have been reported. It has been shown conclusively that under certain conditions of step location, step height, and port height, which govern the velocity of gases at the step by the partially ignited propellant surface or by the igniter gas flow, secondary ignition can occur far downstream of the step. This is very likely to be within the recirculating flow region. The secondary ignition gives rise to two additional flame fronts, one of which spreads backward at a relatively lower velocity, presumably as a result of low reverse velocities present in the separation zone. This phenomenon is likely to play an important role in the starting transient of solid propellant rockets with nonuniform ports.

Nomenclature

a = burn-rate coefficient
C_h = heat-transfer coefficient
d_t = throat diameter
H_p = port height
H_s = step height
n = burn-rate exponent
q = heat flux
r = burn rate
T_f = flame temperature
U_∞ = freestream velocity
V_n = normal velocity
X_f = flame location
X_s = step location
ρ = density

Subscripts

g = gas
p = propellant
w = wall
∞ = freestream condition

Introduction

THE flame-spreading process in a solid rocket motor is known to influence the initial part of the thrust or pressure transient. Flame spreading over a propellant surface is a complex process because the flame-spreading process in a rocket motor is coupled to igniter system, port geometry, chamber gas dynamics, propellant characteristics, location of the initial ignition, and so on. The flame-spreading interval is defined as the time interval between the first ignition of the propellant surface and the ignition of the entire propellant grain.

The mechanism of flame spread apart from being dependant on the thermal characteristics of the propellant, is influenced by the heat-transfer process, which in turn depends on the flow, ambient conditions, and propellant geometry. Normally, flame spread mechanism is assumed to be smooth or continuous. But this is not true in many practical rocket motors with nonuniform ports. For instance, dual-thrust motors (DTM) with a single chamber necessarily have nonuniform port geometry. In such configurations it is very likely that the flow separation, recirculation, and reattachment exist. Such flow separation might also be caused by steep divergences, protrusions over the surfaces, or even by high localized burning. Many segmented rocket motors also have sudden changes in port area along the length. This will alter the convective heat transfer and so the flame spread mechanism. The process of flame spread through such a port, which is an input to any model, remains obscure. This topic has not been studied by anybody so far although prediction of ignition transient has been and continues to be a research topic[1] for more than three decades. In all of the earlier studies, whether theoretical or experimental constant port area configurations are considered because constant port area geometry is a good approximation to a large number of solid rocket motors. In the present study the sudden expansion region is modeled/simulated as a backward-facing step. The flow pattern and heat transfer behind backward-facing steps have been widely studied,[2–6] which can aid in interpretation of the present findings. Recently, similar studies on fuel (PMMA) ignition in a sudden-expansion region have been reported,[7] but there has been none in the context of flame spread over propellant surface. In a previous paper[8] the occurrence of secondary ignition at a downstream point followed by the formation of multiple flame front is reported.

In spite of the massive efforts exerted toward understanding the flame spread mechanism over propellant surface, many problems are still unresolved. In an attempt to resolve some of the problems

Presented as Paper 98-3383 at the AIAA/ASME/SAE/ASEE 34th Joint Propulsion Conference and Exhibit, Cleveland, OH, 13–15 July 1998; received 6 January 1999; revision received 15 March 2000; accepted for publication 3 April 2000.

*Professor, Department of Aerospace Engineering.
†Scientist/Engineer, Propulsion, Vikram Sarabhai Space Centre; sanal@kelnet.xlweb.com.
‡Scientist/Engineer, Aeronautics, Vikram Sarabhai Space Centre.
§Section Head, Launch Vehicle Design Group, Vikram Sarabhai Space Centre.

and in the light of new findings, a substantial revision of the existing idea may be necessary. Such problems of urgency to the rocket motor designers are the starting transient prediction prompted by experience with the solid rocket motors with nonuniform port configurations.

In this paper experimental and numerical studies on flame spread with sudden expansions of ports of solid rocket motors under elevated pressure have been reported. Numerical simulation of flame spread has been carried out using a two-dimensional Navier–Stokes solver.

Literature Review

Paul and Lovine[9] and several others have demonstrated the role of flame spread rate in determining the starting transient of solid rocket motors. Indeed the rate of pressure rise can, to a certain extent, be controlled by altering the surface conditions governing the flame spread. Flame spreading over double-base propellant and propellant ingredients in quiescent atmosphere was studied by McAlevy et al.[10] In the experimental investigations freshly prepared rectangular specimens were mounted in a large vacuum tight chamber and were ignited by a hot wire. Flame-spreading velocity was found to vary directly with pressure and ambient oxygen mass fraction and inversely with the specimen surface smoothness. Raizberg[11] presented an analysis and approximate analytical solution to determine the flame-spreading rate as a function of time. He investigated both convective and radiative heating conditions and concluded that the flame spreading rate must increase with time.

In most cases the flame spreading observed over solid propellant is continuous. However, discontinuous flame spreading has also been observed in some laboratory experiments.[12,13] Peretz et al.[13] found that the flame-spreading rate increases with increasing igniter mass-flow rate and decreasing throat area. The discontinuous flame spreading has been attributed to enhanced radiation heat-transfer delayed reaction in the gas phase, enhanced convective heat transfer, and local surface-roughness condition. Indeed the actual cause may be a combination of the four causes just stated, which is succinctly stated by Kumar and Kuo.[14]

Experimental Method

A laboratory-size, solid propellant, window motor was designed to withstand 60 kg/cm^2. A schematic view of the experimental setup is shown in Fig. 1.

The motor has a chamber of size $250 \times 60 \times 60$ mm. It is fitted with two toughened glass windows, one each on either side to facilitate the cinematographic recording or the event of the flame spreading. At the head end of the motor, a safety valve that can operate at 25 kg/cm^2 is fixed. The ignition is carried out by a thin nichrome wire, which is energized by an ac autotransformer. At the aft end of the motor, a nozzle block assembly is fitted. In the present study ammonium perchlorate-hydroxyl terminated polybutadiene-aluminium propellant ($\rho_p = 1.77$ g/cm^3, $T_f = 3450$ K, $r = 3.47P^{0.35}$, where P is pressure in MPa and r is in mm/s.) with 18% metal and 86% solid loading is used. The propellant sample is inhibited on all sides other than the top surface. The propellant specimen is glued on a variable height wooden plank and mounted in the motor. Metal plates can be fitted on the top wall of the motor to affect changes in port area.

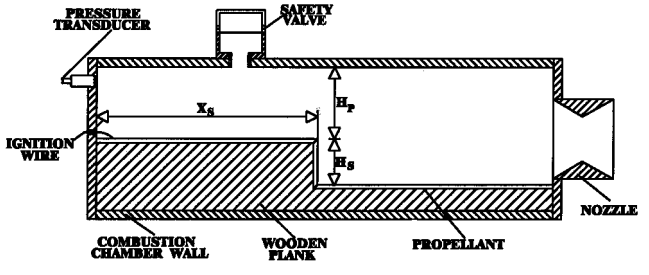

Fig. 1 Schematic of the two-dimensional motor for flame spread studies.

The two parameters of interest are the flame propagation rate and the chamber pressure of the motor. A high-speed camera and a pressure transducer are used for this purpose. The processed film is analyzed in a motion picture analyzer frame by frame. Several problems related to erosion of glass window, illumination of the burning surface, and uniform ignition along the width had to be resolved before obtaining accurate experimental data.

The parameters that are changed are the port height H_p, step height H_s, and the step location X_s, which are shown in Fig. 1. Nearly 40 firings were conducted, and data from only those firings, which gave clear and distinct photographic images, were analyzed. These have been reported in detail in a previous paper.[8]

Data generation, both qualitative and quantitative, is through frame-by-frame analysis of the cine photographic records obtained at a speed of 100 pictures per second. This camera speed is adequate for observing and analyzing the sequence of events during the flame spread at the test conditions. Location of the main flame front X_f at different instants of time t constitute the raw data from which the rate of flame spread, occurrence of secondary ignition, and other information are deduced. In this discussion a reference to secondary ignition implies the formation of additional flame fronts that augment the flame spreading.

It takes a few seconds after the nichrome wire becomes white hot for the first burst of flame, i.e., ignition, to occur. The first flame seems like a hangfire (virtually stationary) at the beginning because in this configuration little convection is present at that stage. The instant when the flame spreading becomes perceptible is arbitrarily denoted as time $t = 0$. This obviously does not alter any derived information like the rate of spread.

Compared to the tests conducted at atmospheric pressure,[15] relatively shorter timescale and higher velocity levels are evident at elevated pressure tests. Some experimental results under elevated pressure tests have been presented earlier,[16] and a detailed discussion is available in Ref. 8.

Qualitatively, in all firings tiny flamelets are observed well ahead of the flame front as in the case of a uniform port configuration, a feature reported by Andoh et al.[12] However, these flamelets do not generate additional moving flame fronts, but are engulfed by the main flame front. When the flow velocities are low enough over a period during which a forward spreading flame approaches the step, the situation may not be too different from the case without a step. Figure 2 shows an example of the case of only forward spread in the presence of a step.

In contrast to the preceding, when the flow rates are sufficiently high upstream of the step, one could expect distinct flow separation. This would be the case when the step is further downstream or the port is narrower. Figure 3 shows a case with a secondary ignition at a downstream region followed by a backward spread of the flame in addition to the normal forward spreading.

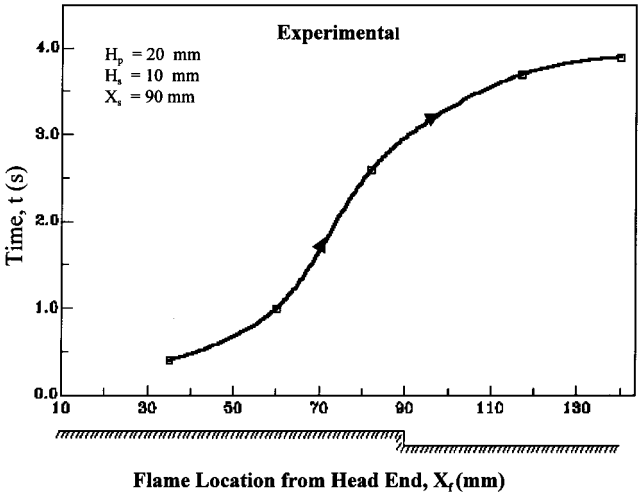

Fig. 2 Example of the case of only forward flame spread in the presence of a step.

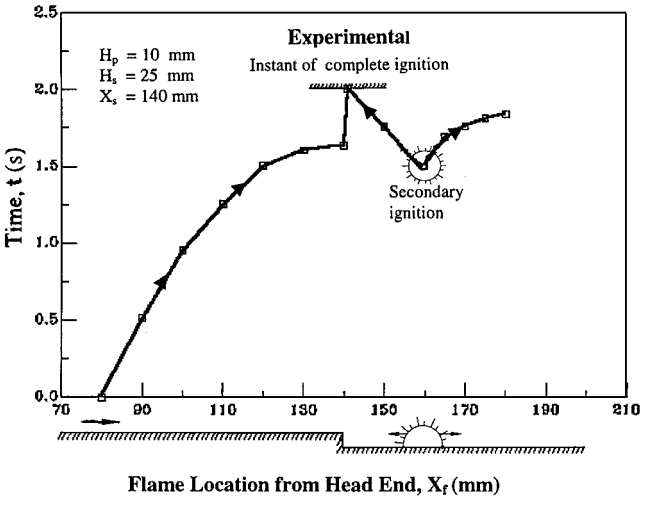

Fig. 3 Case of backward flame spread at higher pressure (peak pressure = 12.6 Ksc).

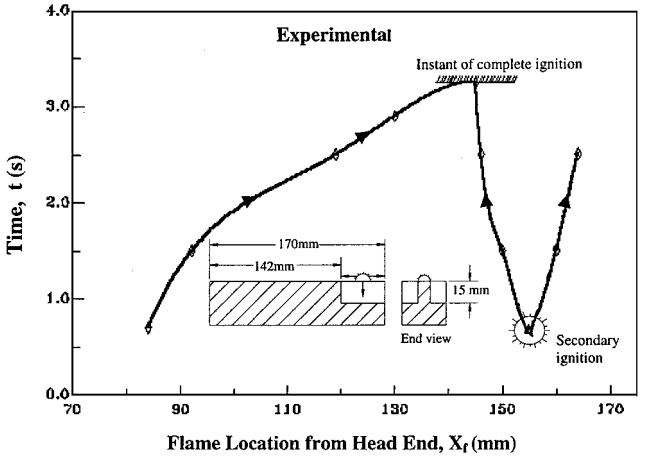

Fig. 4 Case with web downstream of the step. Web configuration in two views in inset (peak pressure = 14.3 Ksc).

In all of the tests, with backward-facing step it is observed that the vertical face of the step is the last part of the specimen to be consumed. Because the propellant thickness and normal burn rate are uniform all over, this is corroborating evidence for the formation of multiple flame fronts.

The phenomena of secondary ignition has been observed with the aid of color video photography, and data recording has been done with the help of cinematography.

Figure 4 shows a flame-spreading phenomenon at high pressures with a grain geometry that includes a thin web downstream of the step. This obviously generates a three-dimensional geometry closer to the DTM grain near the expansion region. The secondary ignition was observed first on the top part of the web followed by flame spread in all directions.

It has been shown conclusively that under certain conditions of step location and port height, which govern the velocity of gases at the step by the partially ignited propellant surface, secondary ignition can occur far downstream of the step. This is very likely to be a region of reattachment of flow. The secondary ignition gives rise to two additional flame fronts, one of which spreads backward at a relatively lower velocity presumably because of the low reverse velocities present around the separation zone. This phenomenon is likely to play an important role in the ignition transient of solid propellant rockets with nonuniform ports. Having proved the concept of secondary ignition, the next step will be to develop a theoretical model for practical applications. These efforts are described in the subsequent sections.

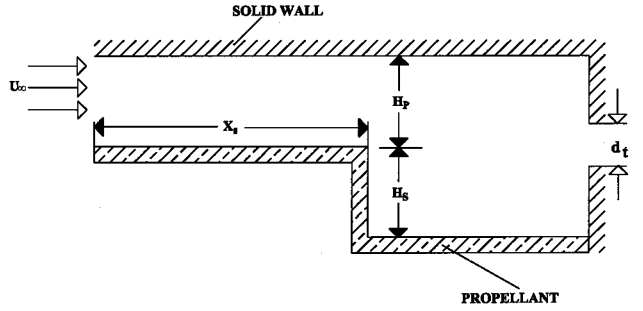

Fig. 5 Idealized two-dimensional model of a solid rocket motor with sudden expasion port.

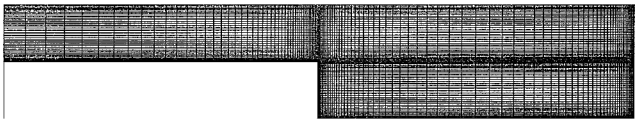

Fig. 6 Grid system in computational region (120 × 80).

Numerical Method of Solution

A detailed numerical simulation of the flame spread and corresponding flowfield in a sudden expansion combustor has also been carried out with the help of a two-dimensional code. This code solves unsteady Reynolds-averaged thin-layer Navier–Stokes equations by an implicit LU-factorization time-integration method. It uses state-of-the-art numerical methods like upwind differencing with Van Leer flux-vector splitting, which are necessary for getting good quality time accurate solutions for practical configurations. An idealized physical model is shown in Fig. 5. This is a good representation of the nonuniform ports of a solid rocket motor.

The system of governing differential equations with boundary conditions is solved using the finite volume method. The viscosity is determined from the Sutherland formula.

An algebraic grid-generation technique is employed to discretize the computational domain. A typical grid system (120 × 80) in the computational region is shown in Fig. 6. The grids are clustered near the solid walls using suitable stretching functions.

The motor parameters and propellant properties including the burning-rate constants are known a priori.

Especially for internal transient problems boundary conditions are very crucial. Treatment of boundary conditions depends up on the problem to be solved. In this analysis initial propellant surface temperature is prescribed, and solid-wall (nonpropellant) temperature is specified as the propellant autoignition temperature. At the solid walls a no-slip boundary condition is imposed. The heat-transfer coefficient $[C_h = 2q_w/(\rho_\infty U_\infty^3)]$ is evaluated from the model, and further propellant surface temperature is determined using Zien's equation.[17]

Burn rate $(r = aP^n)$ is computed based on the local pressure of the cell. For the initial state of low velocities and low pressure rise, one can ignore erosive and transient burn rates.

Using the burn rate r, propellant density ρ_p, and gas density ρ_g, normal velocity caused by propellant burning is given by $V_n = r\rho_p/\rho_g$, and tangential velocities are specified as zero. Step location X_s, step height H_s, and port height H_p in Fig. 5 are chosen to conform with the experimental condition presented in Ref. 8.

Using this model, several test runs were made with different port geometries, inflow conditions, and grids. The Courant–Friedrichs–Lewy number is chosen as 2.0 in all of the computations.

Results and Discussion

The numerical results corresponding to the experimental configuration and propellant properties reproduce many qualitative features such as secondary ignition and backward flame spread. Figures 7a–7c show the velocity distribution of a test case where secondary ignition is evident. In this test case secondary ignition occurred at $t = 0.2058$ s. Reverse flow is discernible, at the upstream of the step,

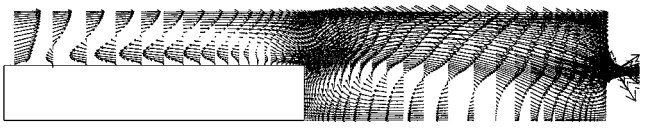

Fig. 7a Velocity distribution before secondary ignition (t = 0.189 s).

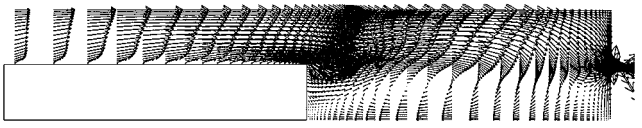

Fig. 7b Velocity distribution at the time of secondary ignition (t = 0.20589 s).

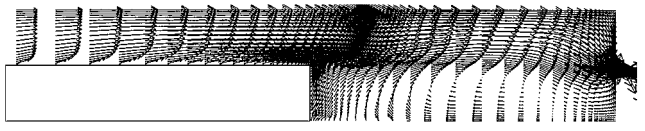

Fig. 7c Velocity distribution after secondary ignition (t = 0.223 s).

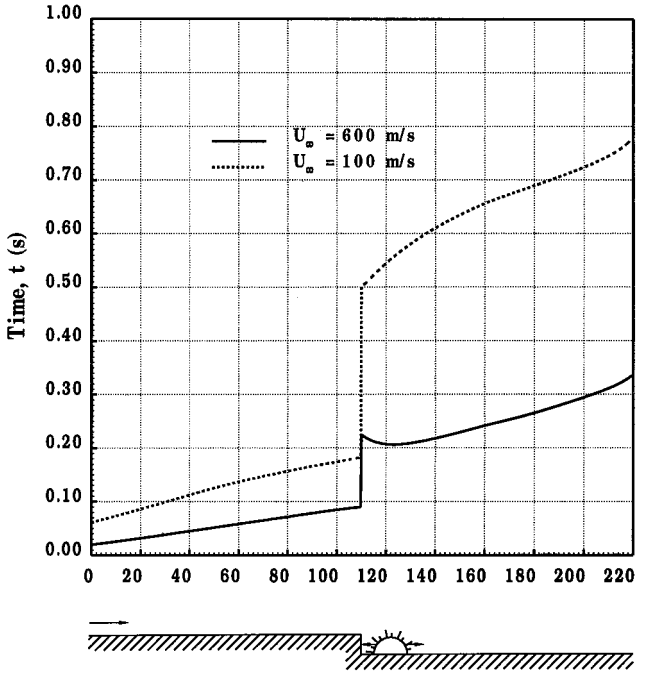

Fig. 8 Numerical prediction of the location of flame fronts at different intervals showing with and without secondary ignition at two different inlet velocities over a same backward-facing propellant surface.

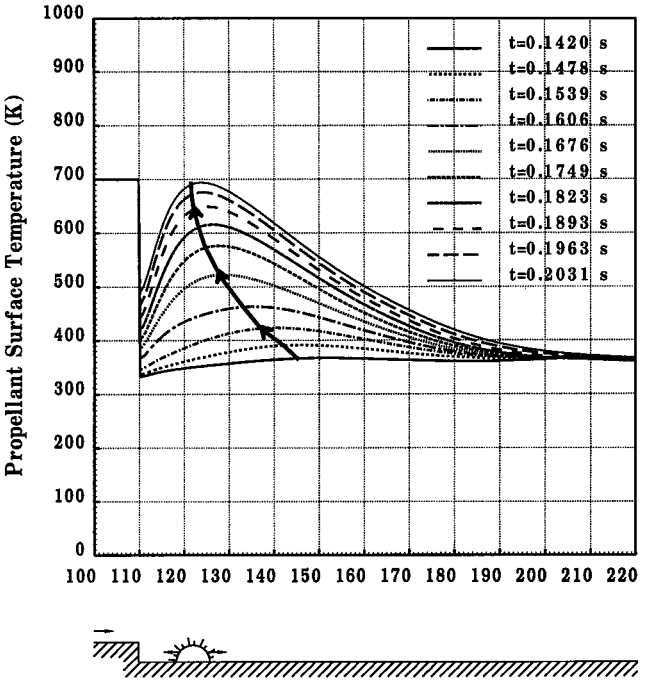

Fig. 9 Numerical prediction of the propellant surface temperature at different intervals showing the shifting of the peak values of the heat flux toward the step.

well before the secondary ignition, and it is apparent at $t = 0.189$ s. This is presented as Fig. 7a. At the time of secondary ignition, the reverse flow at the upstream of the step vanished. This change over has taken place within a short period of time (16.8 ms), and it is visible in Fig. 7b. In this figure recirculation region can easily be recognized. Figure 7c shows the velocity distribution after the secondary ignition ($t = 0.223$ s). At this time flow is established at the upstream of the step; however, reverse flow persists at the downstream of the step. Backward flame spread is prominent during these periods (17.2 ms).

Figure 8 shows the numerical prediction of the location of flame fronts at different intervals in a backward-facing propellant surface at two different inlet velocities. It shows that when the inlet velocity is 100 m/s there is only forward spread and when the inlet velocity is relatively higher (600 m/s) secondary ignition is evident. This indicates that the inflow condition is very crucial for modeling the flame spread mechanism. Figure 9 shows the shifting of the peak values of the heat flux toward the step during the pre-ignition time. This is because of the shifting of the reattachment location itself due to the reverse flow.

The numerical results presented so far in this paper made it possible to examine for the first time a number of factors, which are important in the ignition transient studies of solid rocket motors with nonuniform port configurations. Toward this end, an attempt has been made for the exact prediction of flame spread over a backward-facing propellant surface. Numerical solutions are sensitive to grid distribution. Considerable effort has been directed toward this study.

Figure 10 shows the numerical solutions of a typical test case with the same inflow condition but with three different grid distributions. Although qualitative features of the flowfield are found to be the same, quantitative differences exist between 120×80 and 240×160 grid cases. It can be seen from further grid refinement that between 240×160 and 350×160 grid systems the time of secondary ignition, total period of multiple flame spread, and the total flame-spread time is found to be almost the same even though some difference persists in the location of the secondary ignition. This difference may be caused by the stretching of the grids. In all of the cases, length of the first grid from the solid surface is taken as 0.25 mm. The location of the secondary ignition has large heat-transfer rates; hence, an error in pinpointing the location of secondary ignition can lead to significant errors in predicting the overall ignition transient of solid rocket motors. This is an area that deserves to be examined more carefully.

Considering the computational time for all of the different cases considered, the 240×160 grid distribution is chosen for further parametric study. Figure 11 shows the flame-front locations with time for the case with same port height H_p and step height H_s but with different step locations X_s. It is seen from this figure that when $X_s = 110$ mm secondary ignition is found to be at 1.3 times the step height from the step location. When $X_s = 80$ mm, secondary ignition has been reduced to 0.9 times the step height. It has been observed through this parametric study that when the step location

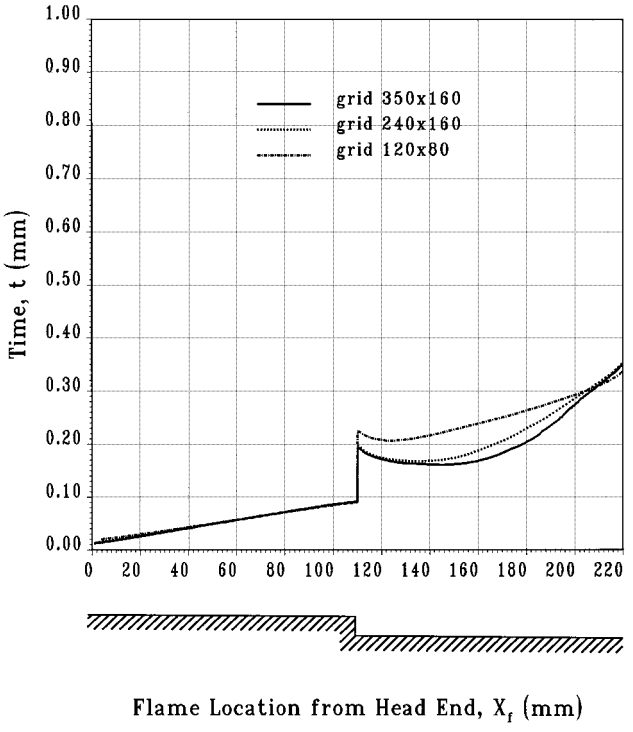

Fig. 10 Numerical solutions of a typical test case with same inflow condition but with three different grid distributions.

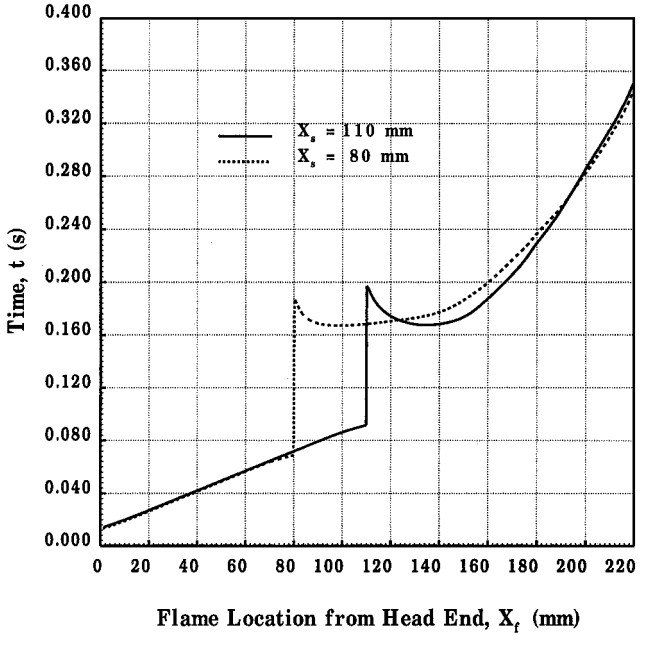

Fig. 11 Numerical prediction of the location of flame fronts at different intervals with same inflow condition, port height, and step height but with two different step locations.

is nearing to the head end, the location of the secondary ignition is tending toward the step location with faster spread rate.

In an another attempt a case with same port height and step location but with different step height does not show any significant difference in the location of the secondary ignition. However delayed secondary ignition is noticed with an increase in step height. This can be seen in Fig. 12.

It has been observed through several comparisons that, with the same inflow conditions and propellant properties, velocity distributions are different for different port geometries during the flame-spreading period. Hence, it has been concluded that, apart from the propellant properties and inflow conditions, the inclusion of the port

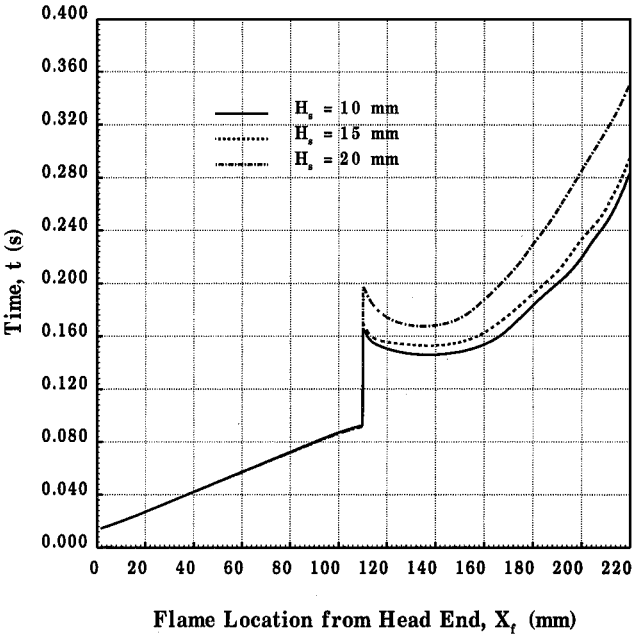

Fig. 12 Numerical prediction of the location of flame fronts at different intervals showing the variation of secondary ignition time with same inflow condition, port height, and step location but with three different step heights.

geometry in the model is also important for the accurate prediction of the flame spread mechanism.

For the different configurations tested in the present experimental work, the peak Reynolds numbers based on step height are estimated to be between 6×10^3 and 4×10^4 at the propellant flame temperature. At these turbulent Reynolds-number ranges, the reattachment point is known to lie at least three times the step height away from the foot of the step. However the zone of secondary ignition for many tests is around 0.8–3.0 times the step height. Therefore one can conclude that the secondary ignition occurs inside the recirculation bubble. The preheating of the propellant in this zone before the arrival of the flame at the sudden expansion also appears important.

The separated flow characteristics such as size of the separation bubble, flow redevelopment, and heat transfer in the recirculation region are known to be dependent on Reynolds number upstream of the step and step height. During the flame-spreading process, the Reynolds number at the top of the step gradually increases as the main flame front advances, attaining a maximum as the flame covers the entire propellant surface before the step. The flame spread being a transient phenomenon, the heat-transfer coefficient gradually increases with time. Hence, ignition of a larger propellant surface area produces more hot gases, which increase the amount of heat transferred to the unburnt propellant surface by convection. Thus, the rate of spread at a given distance or time is increased by increasing the ignition area. As the flame spread rate increases, preheating increases, and the spread becomes accelerative.

In the numerical study different Reynolds numbers are considered. The two cases presented in Fig. 8 with a given Reynolds number (3×10^4) show that high inlet velocity will cause reduction of the effective time for the complete ignition of the propellant surface. Secondary ignition and multiple flame fronts are also observed in one case where inlet velocity is relatively higher, and in the other case, at low velocity, the flame spread is observed as continuous even in the presence of a step. These features are observed experimentally and presented in Figs. 2 and 3. In the experimental conditions port heights are changed for getting different flow velocities. Hence, the formation of a multiple flame front has been observed at different experimental conditions too.

In the numerical studies when the time step increases, the peak value of the heat flux is shifting toward the step location. A case reported here shows (Fig. 9) that the peak temperature zone is located

within the recirculation bubble. It is inferred from these studies that the recirculation region will favour secondary ignition.

The implication of the secondary ignition can be quite serious for a practical rocket. One secondary ignition would result in two additional flame fronts, one spreading forward and the other backward. This effect will be further accentuated in the case of star grain downstream of sudden expansion where the star points generate multiple flame fronts. The effective time required for the complete burning surface area to be ignited comes down drastically giving rise to a high pressurization rate (dP/dt) in the second phase of ignition transient. This in effect could lead to a hard start of the rocket motor.

Conclusions

Although the experimental investigations of flame spread mechanism proved conclusively the formation of secondary ignition, it is difficult to separate the effects of geometry from the inlet flow conditions on the formation of multiple flame fronts. This ambiguity has been overcome by the present model. The detailed parametric study has revealed that the proposed model will be able to reasonably predict the condition of the flow separation and reattachment at different environmental conditions and material properties at a given initial and boundary condition. Hence, the model will be useful for the designer to design a solid rocket motor in the thrust transient point of view.

It may be conjectured from this experience that the phenomenon of flow separation and reattachment could also modify the nature of erosive combustion, which is also a consequence of convective heat transfer. This also adds to the complexity of the ignition transient. This calls for a reexamination of the existing concept of solid propellant motor ignition and subsequent flame spread before embarking on the formulation of a new model and a code of solution.

The experience gained through this code has made it possible to develop a three-dimensional version of the model for handling more complex geometries for practical applications.

References

[1]Luke, G. D., Eager, M. A., and Dwyer, H. A., "Ignition Transient Model for Large Aspect Ratio Solid Rocket Motors," AIAA Paper 96-3273, July 1996.

[2]Krall, K. M., and Sparrow, E. M., "Turbulent Heat Transfer in the Separated, reattached, and Redevelopment Regions of a Circular Tube," *Trans. ASME Journal of Heat Transfer*, Vol. 88, No. 2, Series C, 1966, pp. 131–136.

[3]Aung, W., "An Experimental Study of Laminar Heat Transfer Downstream of Backsteps," *Trans. ASME Journal of Heat Transfer*, Vol. 105, No. 4, Nov. 1983, pp. 823–829.

[4]Amano, R. S., Jensen, M. K., and Goel, P., "A Numerical and Experimental Investigation of Turbulent Heat Transport Downstream from an Abrupt Pipe Expansion," *Trans. ASME Journal of Heat Transfer*, Vol. 105, No. 4, 1983, pp. 862–869.

[5]Aung, W., Baron, A., and Tsou, F.-K., "Wall Independency and Effect of Initial Shear-Layer Thickness in Separated Flow and Heat Transfer," *International Journal of Heat and Mass Transfer*, Vol. 28, No. 9, 1985, pp. 1757–1771.

[6]Sparrow, E. M., Kang, S. S., and Chuck, W., "Relation Between the Points of Flow Reattachment and Maximum Heat Transfer for Regions of Flow Separation," *International Journal of Heat and Mass Transfer*, Vol. 30, No. 3, 1987, pp. 1237–1245.

[7]Yang, Jing-Tang, and Cliff, Y. Y. Wu., "Controlling Mechanisms of Ignition of Solid Fuel in a Sudden Expansion Combustor," *Journal of Propulsion and Power*, Vol. 11, No. 3, 1995, pp. 483–488.

[8]Raghunandan, B. N., Madhavan, N. S., Sanjeev, C., and Sanal Kumar, V. R., "Studies on Flame Spread with Sudden Expansions of Ports Under Elevated Pressure," *Defence Science Journal*, Vol. 46, No. 5, 1996, pp. 417–423.

[9]Paul, B. E., and Lovine, R. L., "Propellant Surface Flame Propagation in Rocket Motors," AIAA Paper 64-125, Jan. 1964.

[10]McAlevy, R. F., Magee, R. S., Wrubel, J. A., and Horowitz, F. A., "Flame Spreading over the Surface of Igniting Solid Rocket Propellants and Propellant Ingredients," *AIAA Journal*, Vol. 5, No. 2, 1967, pp. 265–271.

[11]Raizberg, B. A., "Physical Basis and Mathematical Model of the Propagation of a Flame over the Surface of a Solid Propellant During Ignition," *Combustion Explosion and Shock Waves*, Vol. 4, No. 4, 1968, pp. 330–335.

[12]Andoh, E., Mizomoto, M., and Ikai, S., "Flame Spreading over the Surface of a Solid Propellant, Part 1: Experimental Results," *Combustion Science and Technology*, Vol. 26, Nos. 3 and 4, 1981, pp. 135–146.

[13]Peretz, A., Kuo, K. K., Caveny, L. H., and Summerfield, M., "Starting Transient of Solid Propellant Rocket Motors with High Internal Gas Velocities," *AIAA Journal*, Vol. 11, No. 12, 1973, pp. 1719–1727.

[14]Kumar, M., and Kuo, K. K., "Flame Spreading and Overall Ignition Transient," *Fundamentals of Solid Propellant Combustion*, edited by K. K. Kuo and M. Summerfield, Progress in Astronautics and Aeronautics, Vol. 90, 1983, pp. 305–360.

[15]Jaganathan, J., and Raghunandan, B. N., "Flame Spread over a Propellant Surface with a Backward Step," *Proceedings of the XII National Conference on IC Engines and Combustion*, Tata McGraw-Hill Pub. Co. Ltd., New Delhi, India, 1994, pp. 346–351.

[16]Raghunandan, B. N., Madhavan, N. S., Sanjeev, C., and Sanal Kumar, V. R., "Studies on Flame Spread with Sudden Expansions of Ports Under Elevated Pressure. Abstract," *International Seminar on High Energy Materials*, High Energy Materials Society of India (HEMSI), Pune, India, 1996, p. 94.

[17]Zien, T. F., "Integral Solution of Ablation Problems with Time-Dependent Heat Flux," *AIAA Journal*, Vol. 16, No. 12, 1978, pp. 1287–1295.